UNITED STATES DEPARTMENT OF THE INTERIOR

GEOLOGICAL SURVEY

Preliminary investigation of the elemental variation and

diagenesis of a tabular uranium deposit, La Sal mine,

San Juan County, Utah

By

Robert A. Brooks and John A. Campbell

Open-File Report 76-287

1976

Contents

Illustrations

Tables

Preliminary investigation of the elemental variation and
diagenesis of a tabular uranium deposit, La Sal mine,
San Juan County, Utah

By Robert A. Brooks and John A. Campbell

ABSTRACT

Ore in the La Sal mine, San Juan County, Utah, occurs as a
typical tabular-type uranium deposit of the Colorado Plateau.
Uranium-vanadium occurs in the Salt Wash Member of the Jurassic
Morrison Formation.

Chemical and petrographic analyses were used to determine
elemental variation and diagenetic aspects across the orebody.
Vanadium is concentrated in the dark clay matrix, which constitutes
visible ore. Uranium content is greater above the vanadium zone.
Calcium, carbonate carbon, and lead show greater than fifty-fold
increase across the ore zone, whereas copper and organic carbon show
only a several-fold increase. Large molybdenum concentrations are
present in and above the tabular layer, and large selenium
concentrations occur below the uranium zone within the richest
vanadium zone. Iron is enriched in the vanadium horizon. Chromium
is depleted from above the ore and strongly enriched below. Elements
that vary directly with the vanadium content include magnesium, iron,
selenium, zirconium, strontium, titanium, lead, boron, yttrium, and
scandium.

The diagenetic sequence is as follows: (1) formation of secondary
quartz overgrowths as cement; (2) infilling and lining of remaining
pores with amber opaline material; (3) formation of vanadium-rich clay
matrix, which has replaced overgrowths as well as quartz grains;
(4) replacement of overgrowths and detrital grains by calcite;
(5) infilling of pores with barite and the introduction of pyrite
and marcasite.

1

INTRODUCTION

The La Sal mine is located 1.6 km east of the small town of La Sal, in northeastern San Juan County, Utah (fig. 1). It can be reached from Moab, Utah, by taking U.S. Highway 160 38 km south to Utah State Highway 46, then following Highway 46 about 16 km east to La Sal.

This mine was examined as part of a reconnaissance study of tabular uranium-vanadium ore deposits of the Colorado Plateau. Samples were collected along traverses that transected obvious orebodies; however, the orebodies were not mapped in detail. The representativeness of the sample suite described has not been determined; however, the data derived from the sample suite are similar to data derived from other uranium deposits on the Colorado Plateau as well as from other districts.

Several people have aided with different phases of this work. Thanks are due to R. P. Fischer and J. Ridgely of the U.S. Geological Survey, Denver, and to C. E. Nichols of Union Carbide Corporation.

Structural setting

The geology of the area in the vicinity of the La Sal mine has been described by Carter and Gualtieri (1965). The mine is located within a structurally complex area. Salt from the Paradox Member of the Pennsylvanian Hermosa Formation locally has been diapirically injected into a series of northwest-southeast-trending salt anticlines. Faulting accompanying these intrusions and solution features of the salt anticlines have added to the complexity of the area (fig. 2). The La Sal mine lies on the south flank of the Pine Ridge salt anticline and on the north flank of the East Coyote Wash syncline.

Twelve km to the east of the La Sal mine, a considerable amount of uranium-vanadium mining took place along the La Sal Creek Mineral Belt (Carter and Gualtieri, 1965). The La Sal Creek Mineral Belt lies on the north side of the Pine Ridge salt anticline, and very little mining activity has occurred on the south side. The La Sal mine lies along a straight line extension of the La Sal Creek Mineral Belt, but is separated from the belt (as defined by Carter and Gualtieri, 1965) by a large solution-collapse area on the crest of the salt anticline.
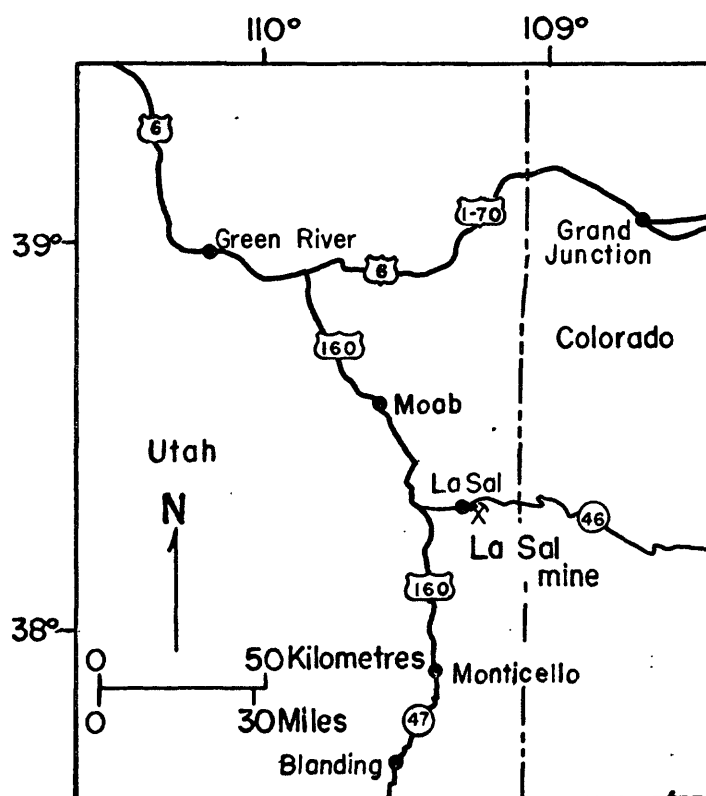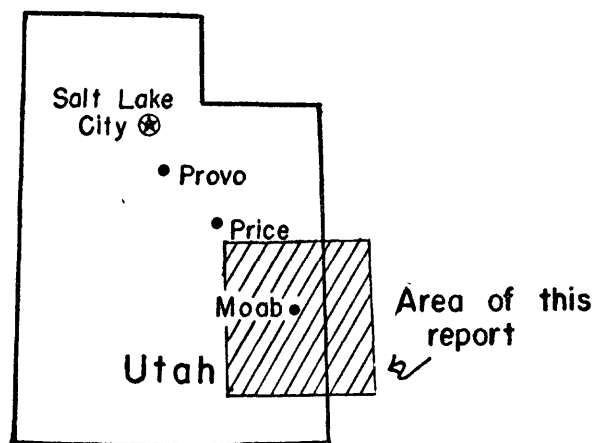
Figure 1.--Index and location map of the
La Sal mine area, San Juan County, Utah.

3

Figure 2. Generalized structural map of the La Sal Mine and La Sal Creek Mineral Belt
(After Carter and Gualtieri, 1965)

$\dfrac{U}{D}$ ——————— Fault (Dashed where approximately located; dotted where concealed. U, upthrown side; D, downthrown side.)

———————— Outline of area where bedrock has collapsed by solution of underlying salt mass.

▲———————— Anticline showing crestline and direction of plunge.

◄►———————— Syncline showing troughline and direction of plunge.

∴∵ Area underlain by uranium–vanadium deposit.

4
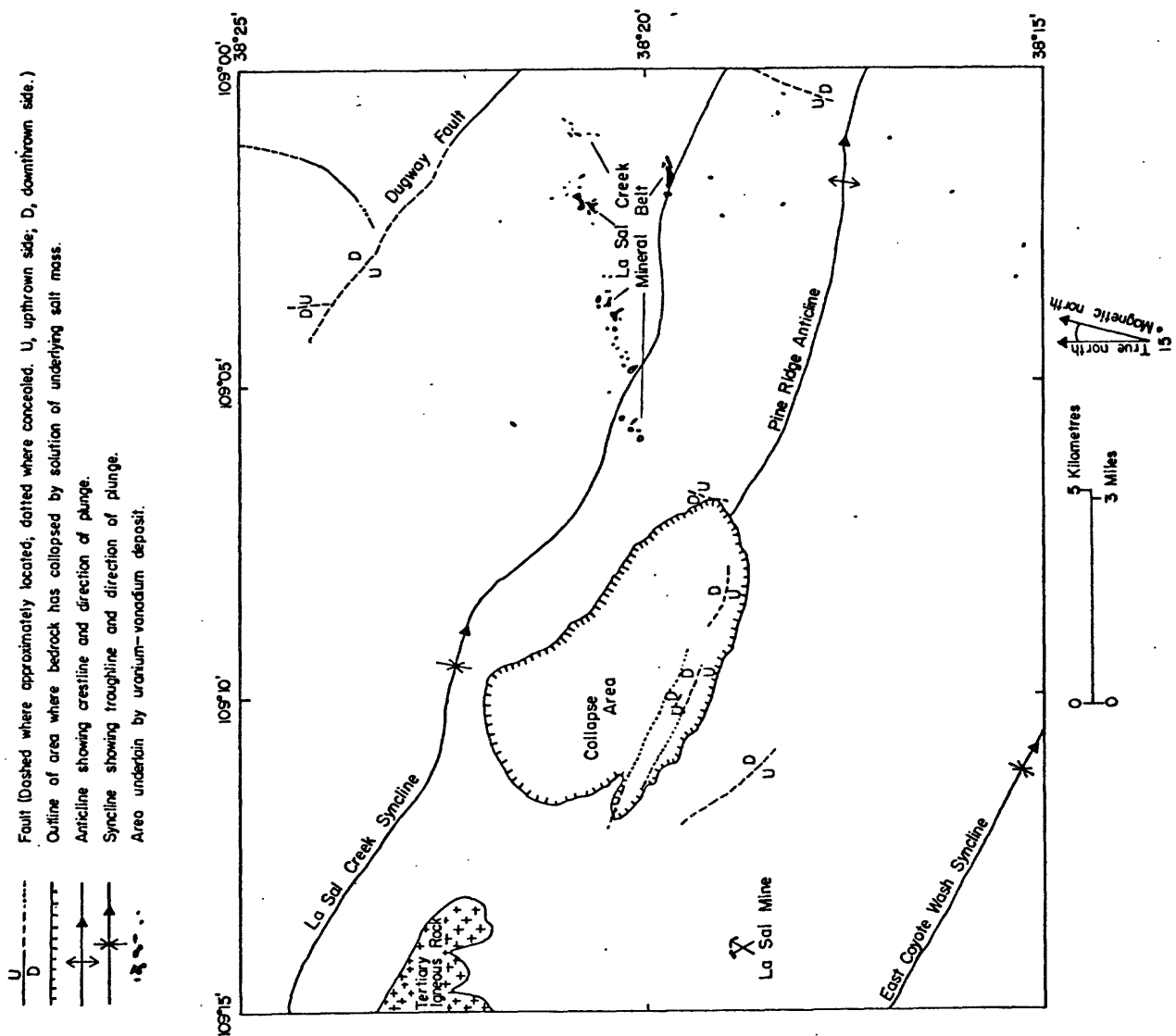
The possibility of such a western extension of the La Sal Mineral Belt
was suggested by Carter and Gualtieri (1965).

Stratigraphic setting

The ore in the La Sal mine occurs in the fluvial sandstones of
the Salt Wash Member of the Jurassic Morrison Formation. The Salt
Wash is composed of a sequence of interbedded fine-grained sandstones
and siltstones. Three recognizable sandstone layers within the
member form erosion-resistant ledges separted by intervening softer
siltstones. The upper layer or "third ledge" is usually the
ore-bearing layer. The ore in the La Sal mine occurs as a 25-cm-thick
tabular body that parallels bedding within the "third-ledge"
sandstone layer.

Location of samples

Ore occurs in a small raise above the main haulage way and is in
the uppermost portion of the third-ledge sandstone. A visibly distinct,
stained, horizontal layer is thought to delineate the vertical extent
of the orebody. A suite of eight grab samples was collected across
the stained layer in order to determine the geochemical and mineralogic
nature of the mineralization and alteration. Samples were centered
every 15 cm (6 in.) along a traverse perpendicular to the stained layer.
Samples 9 through 12 were collected above the stained layer, samples 13
through 15 were collected within the layer, and sample 16 was taken
below the stained layer. Sampling was restricted by the dimensions of
the mine.

ANALYTICAL RESULTS

Chemical

Figure 3 shows the uranium and vanadium content of the samples.
It can be seen that the staining mentioned above indicates the position
of the vanadium ore but not of the uranium-rich sandstone. The vanadium
concentration reaches 15,000 ppm in the stained zone, but the uranium
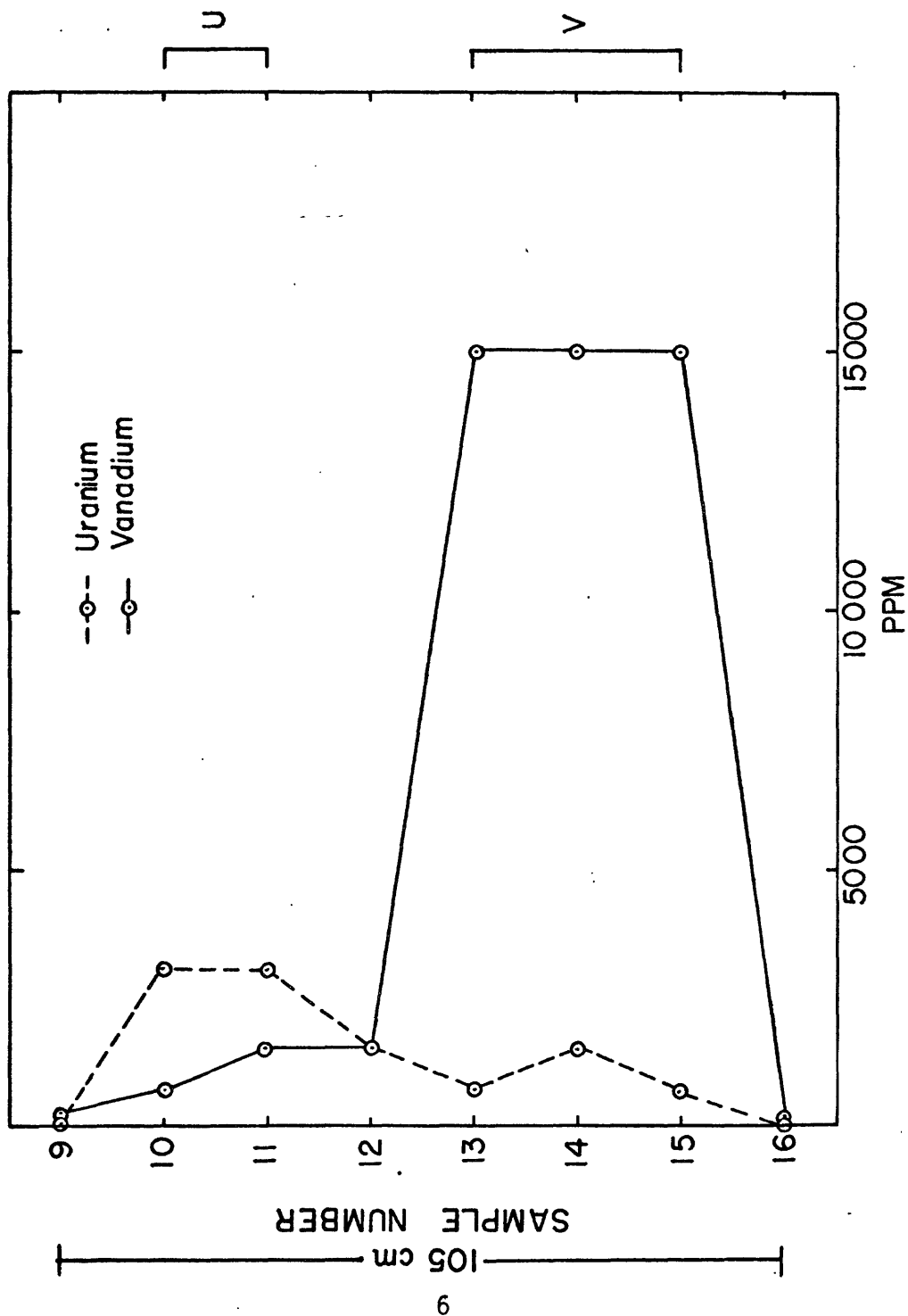concentration remains quite low. The uranium is more concentrated above

5

Figure 3.--Uranium and vanadium content of samples. Samples taken over 105 cm. intervals. Brackets refer to samples with maximum concentrations of uranium and vanadium.

6

the vanadium ore layer, where it reaches a maximum concentration of 3,000 ppm. Separation of the uranium and vanadium zones of maximum mineralization is quite common in the uranium-vanadium ores of the Colorado Plateau, and sampling on the basis of color and staining can result in sampling the vanadium and missing the uranium ore (R. P. Fischer, oral commun., 1975).

Results of chemical analysis by emission spectroscopy of the sample suite are given in table 1. Most elements analyzed show significant variation across the ore layer. The concentrations of calcium, carbonate carbon, and lead show greater than fifty-fold increases, whereas copper and organic carbon show only several-fold increases. A good deal of variation, especially where the concentration of an element varies directly with vanadium content, is due to the facts that in the vanadium-rich zone the detrital sand grains are corroded and the interstitial pore spaces are filled with a matrix composed of compounds of several elements. In contrast, the vanadium-poor sands have not undergone corrosion, but rather have developed more normal interstitial quartz and calcite cements and overgrowths.

Although not statistically significant, some elements seem to vary directly with the vanadium content: magnesium, iron, selenium, zirconium, strontium, titanium lead, boron, yttrium, and scandium. Table 2 gives the linear-regression correlation matrix of all the elements measured.

Heavy minerals

Table 3 and figure 4 show the content of the heavy-mineral fraction as determined by X-ray diffraction. There is a significant decrease in the relative amounts of heavy minerals from top to bottom in the sample suite. Pyrite is present in all samples, but no other heavy minerals are ubiquitous. The ore minerals uraninite, coffinite, cuprosklodowskite, and epiianthinite are found in one or two samples. Lead minerals clausthalite and galena are also present. Samples below the ore contain a normal suite of detrital heavy minerals including brookite, zircon, anatase, and rutile, but these minerals are not found in the upper zones.

7

Table 1.--<u>Chemical analysis of whole-rock samples across tabular ore layer</u>

[All data were determined by analytical laboratories, U.S. Geological Survey. Except as noted, all elements were determined by a semiquantitative six-step spectrographic technique; L. A. Bradley, analyst. Total Fe was determined by atomic absorption; W. Mountjoy, analyst. Total carbon was determined by a combustion-conductometric technique; V. E. Shaw, analyst. Carbonate carbon was determined by a H_3PO_4 digestion-gasometric technique; T. L. Yager, analyst. Organic carbon was determined by differences.

[1]N = Not detected or at limit of detection.

[2]L = Detected, but below limit of determination.]

Sample No.------,---	9-11-7	10-11-7	11-11-7	12-11-7	13-11-7	14-11-7	15-11-7	16-11-7
U percent	N[1]	0.30	0.30	0.15	0.07	0.15	0.07	N
V percent	0.02	.07	.155	.15	1.50	1.50	1.50	0.015
Total Fe as Fe_2O_3 (%)	1.29	.39	.74	.22	1.63	2.19	1.08	.41
Mg percent	.50	.10	.07	.07	.70	.70	.70	.15
Ca percent	2.00	.15	.03	.03	.15	.15	.15	.50
Ti percent	.02	.07	.05	.05	.15	.20	.15	.03
Total C as C, percent	1.61	.42	.36	.44	.21	.84	.66	1.02
Carbonate C as C, percent	1.42	.07	.01	<.01	.02	.02	.03	.34
Organic C as C, percent	.2	.4	.4	.4	.2	.8	.6	.7
Mn ppm	200	70	20	30	70	70	30	150
Ag ppm	N	.7	N	N	1.5	.7	1.0	N
B ppm	L[2]	L	L	L	20	20	20	L
Ba ppm	100	1500	500	200	150	200	200	100
Be ppm	N	N	N	N	2	3	1.5	N
Co ppm	15	30	10	L	15	30	10	N
Cr ppm	3	1.5	2	L	15	15	15	100
Cu ppm	15	7	5	15	7	7	30	7
Mo ppm	30	50	N	N	3	5	5	N
Ni ppm	L	10	L	L	15	15	7	L
Pb ppm	15	20	50	15	1500	700	1500	15
Sc ppm	N	N	N	N	5	7	5	N
Se ppm	19	32	22	9.2	1840	370	1430	6.2
Sr ppm	15	10	15	7	70	150	100	15
Y ppm	N	N	L	10	15	30	20	N
Zr ppm	15	70	50	30	150	100	150	30

Table 2.--Correlation matrix of whole-rock elemental concentrations

	Mg	Ca	Ti	Mn	Ag	Ba	Co	Cr	Cu	Mo	Ni	Pb	Sr	U	V	Zr	Se	Fe$_2$O$_3$	TC	CO$_3$	OC
Ca	.16																				
Ti	.77	-.45																			
Mn	.09	.88	-.43																		
Ag	.80	-.27	.78	-.26																	
Ba	-.45	-.27	-.13	-.23	-.30																
Co	.32	-.03	.50	-.01	.14	.56															
Cr	-.12	.02	-.19	.41	-.09	-.31	-.42														
Cu	.38	.13	.15	-.13	.22	-.28	-.28	-.17													
Mo	-.40	.36	-.47	.40	-.52	.72	.39	-.13	-.11												
Ni	.64	-.34	.85	-.21	.72	.15	.71	-.19	-.22	-.13											
Pb	.83	-.29	.80	-.33	.96	-.30	.10	-.10	.43	-.53	.63										
Sr	.82	-.25	.94	-.24	.65	-.30	.44	-.07	.22	-.51	.72	.71									
U	-.52	-.52	-.03	-.60	-.33	.77	.41	-.49	-.40	.24	.07	-.33	-.19								
V	.87	-.35	.95	-.36	.90	-.32	.30	-.14	.30	-.58	.76	.93	.91	-.24							
Zr	.72	-.47	.86	-.47	.92	-.04	.29	-.16	.30	-.42	.74	.95	.72	-.07	.91						
Se	.74	-.26	.67	-.28	.97	-.27	.02	-.09	.37	-.48	.58	.97	.54	-.34	.83	.92					
Fe$_2$O$_3$	.87	.15	.75	.10	.62	-.38	.51	-.19	-.03	-.42	.71	.58	.83	-.27	.76	.53	.48				
TC[1]	.18	.89	-.33	.86	-.37	-.37	-.04	.27	.19	.25	-.36	-.32	-.04	-.58	-.28	-.49	-.38	.18			
CO$_3$	.10	1.00	-.51	.88	-.33	-.25	-.06	.03	.11	.38	-.40	-.35	-.31	-.31	-.41	-.52	-.31	-.09	.88		
OC[2]	.08	-.38	.39	-.15	-.08	-.12	.09	.50	.05	-.27	.12	.04	.53	-.03	.26	.11	-.15	.13	.09	-.39	

[1]TC, total carbon.
[2]OC, organic carbon.

9

Table 3.--Heavy-mineral content of samples

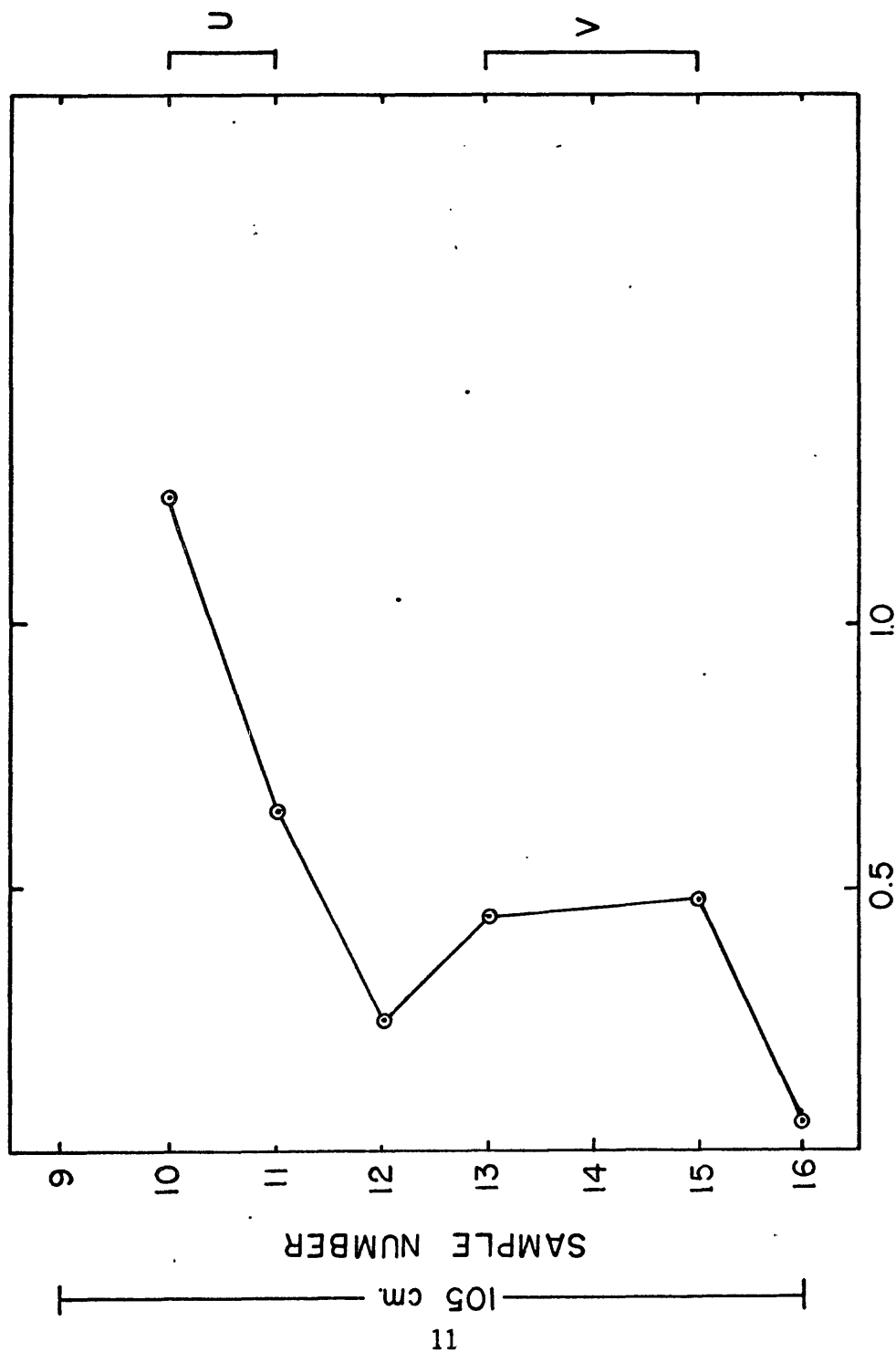| Sample No.	9-11-7	10-11-7	11-11-7	12-11-7	13-11-7	14-11-7	15-11-7	16-11-7
Coffinite		X					X	
Barite		X						
Apatite		X						
Pyrite		X	X		X		X	
Cuprosklodowskite			X					
Epi-ianthinite				X				
Clausthalite					X			
Brookite					X			X
Sphalerite							X	
Uraninite							X	
Zircon								X
Rutile								X
Anatase								X

Figure 4.—Heavy mineral content of samples, in percent.
Brackets refer to samples with maximum concentrations of uranium and vanadium. Samples taken over 105 cm interval.

11

Petrography

The petrographic relations within the Morrison Formation and within selected areas of the Salt Wash Member have been described by several authors (Hausen, 1959; Cadigan, 1967; Shawe, 1968; Hafenfield and Brookins, 1975). The average mineral composition of the Salt Wash Member sandstones, based on 202 samples throughout the Colorado Plateau, is 71.4 percent quartz, 4 percent quartz overgrowth, 5.8 percent chert, 5.8 percent potassium-feldspar and plagioclase, and 13 percent calcite (Cadigan, 1967).

Composition

Table 4 shows the mineral composition of the La Sal mine suite of samples. The data are derived from point counts of 100 grains for each sample. This suite is similar to the average Salt Wash Sandstone composition except that it is generally depleted in calcite. In the vanadium-rich samples, the detrital grains have been corroded and the original grain composition is hard to determine.

The greatest variation in composition is in the amount of matrix material. Matrix material here is rather loosely defined as an interstitial clay, which in plain light is dark brown to black. This matrix comtains vanadium mica, roscoelite, and illite, with minor amounts of kaolinite, chlorite, and mixed-layered illite-montmorillonite. The presence of several of the elements in table 2 also correlates with the abundance matrix material. The process of emplacement of the matrix has been quite corrosive to the original grains, having removed most of the smaller grains, embayed larger quartz grains, and removed secondary overgrowths (fig. 5).

12

Table 4.--Mineralogic composition of samples

[✓ Minerals present in amount less than 1 percent]

| Sample No.-----	9	10	11	12	13	14	15	16
Common quartz--	51	61	57	56	35	41	65	61
Meta-quartzite------	8	8	7	1	3	2	3	10
Quartz overgrowths----	2	8	20	14	✓	0	✓	1
Chert----------	0	✓	✓	1	2	2	1	1
Sedimentary rock fragments-	0	1	1	2	5	5	✓	2
Volcanic rock fragments-	4	2	1	✓	✓	✓	1	3
Feldspar-------	8	3	3	2	2	3	2	3
Calcite--------	15	1	✓	0	✓	0	1	4
Pyrite---------	0	0	0	0	0	0	3	1
Heavies--------	1	1	2	✓	3	1	✓	✓
Matrix---------	1	0	1	5	43	43	18	2
Opal-----------	-	4	2	4	1	1	✓	4
Void-----------	10	11	6	14	6	1	3	8
Other----------	✓	✓	✓	✓	✓	1	3	✓
Total	100	100	100	100	100	100	100	100

13

Figure 5.--Photomicrographs showing sandstone textures.
a Sample 16-11-7 shows detrital texture only slightly
modified by alteration (10X).
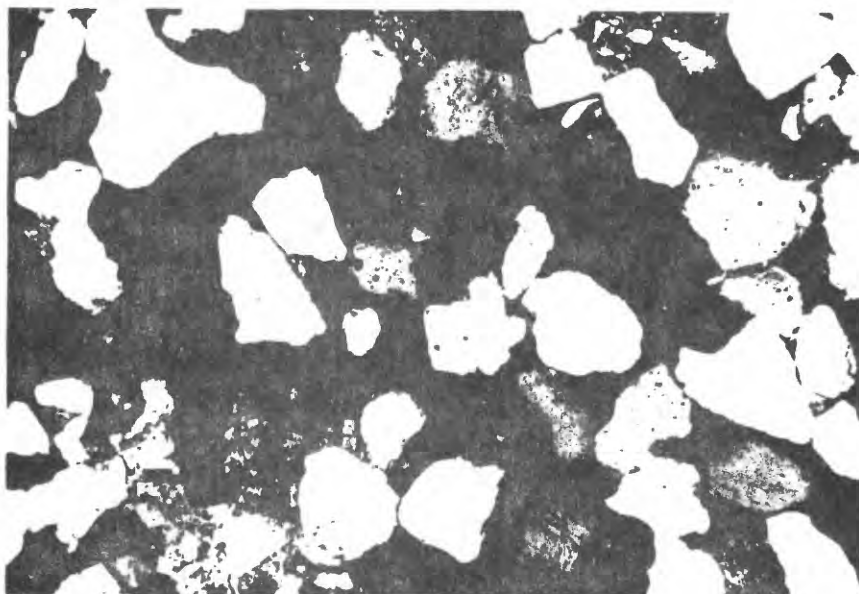
b. Sample 13-11-7 shows destruction of detrital components
by ore emplacement (10X).
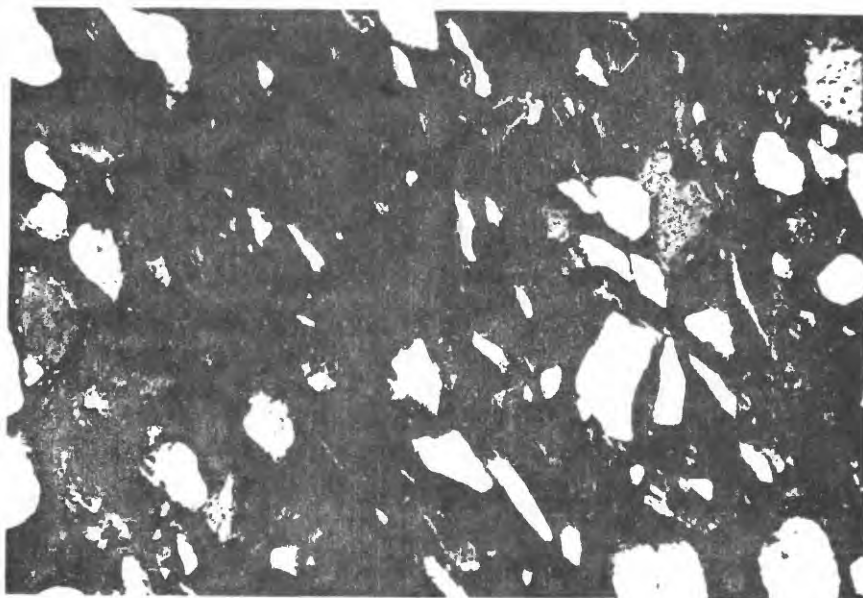
Diagenesis

Table 5 shows the general distribution of diagenetic events
as determined from thin sections. A similar sequence of events is
visible in all samples; however, not all of the events are apparent in
all samples. The sequence begins with the formation of secondary
overgrowths on the quartz grains. This secondary quartz is the primary
cementing agent in most of the samples. The second event is the
introduction of an amber material, which is primarily opal but contains
significant amounts of Fe, Ti, and other elements, and which fills or
lines voids left after cementation. The composition of this material
is presently being analyzed and will be reported later. The third
event is the formation of the dark clay-matrix material containing
montroseite and other vanadium minerals. Some minor clay minerals,
including illite in some samples and kaolinite in others, may have
formed earlier. In samples 13, 14, and 15, the dark-clay matrix is so
abundant that it obscures evidence of previous events. This matrix
material is followed by the introduction of calcite, which grows in the
amber material and replaces all other grains and overgrowths. Filling
of remaining pores by varite occurs next. In the samples below the ore,
a final event is the introduction of pyrite and marcasite.

DISCUSSION OF RESULTS

Harshman (1974) discussed the distribution of elements in
roll-type uranium deposits in Wyoming, Texas, and South Dakota. In
addition to uranium, four other elements were particularly significant
in terms of the roll model. Figure 6 shows the distribution of the
four most significant elements in roll-type deposits plus the
distribution of pyrite, which is interpreted to represent all ferrous
iron compounds. Selenium and vanadium occur on the altered or oxidized
side of the maximum uranium peak, and molybdenum and pyrite occur on
the unaltered or reduced side of the uranium ore zone. Shawe (1966)
noted the similarity of distribution of eU, U, V, Cu, Pb, Zn, As, and
Se in both tabular and roll-type uranium deposits and concluded that
both types of deposits were formed by precipitation at the interface
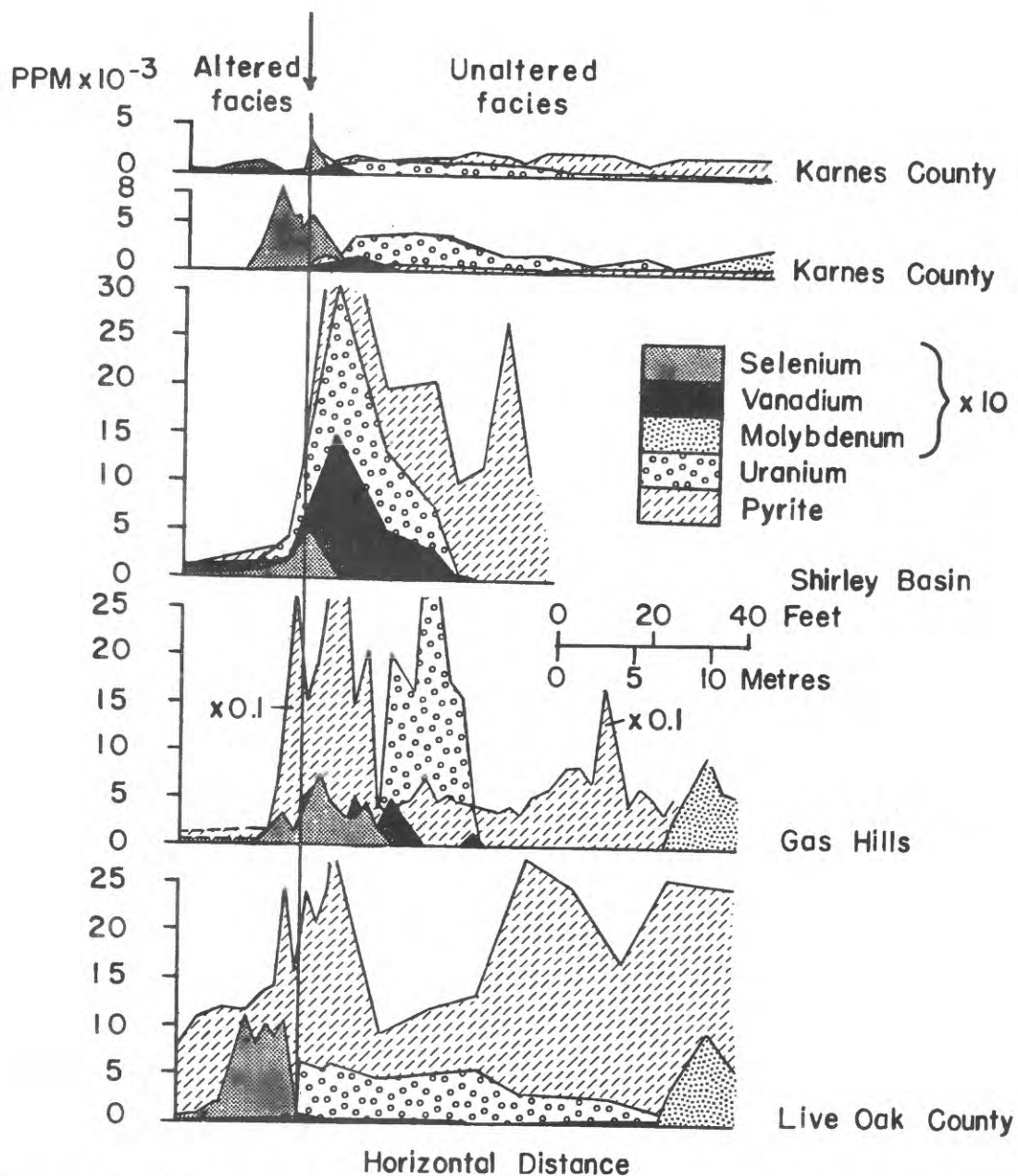between two solutions of different composition. In the La Sal suite

Figure 6.--Distribution of elements in some roll-type uranium
deposits. (Harshman, 1974).

Table 5.--Distribution of diagenetic events

Sample No.	Order of diagenetic event							
	9-11-7	10-11-7	11-11-7	12-11-7	13-11-7	14-11-7	15-11-7	16-11-7
Quartz overgrowth	X	X	X	X	X		X	X
Early clay formation	X			X	X	X	X	
Amber	X	X	X	X	X	X	X	X
Matrix opaque ore	X	X	X	X	X	X		
Calcite	X	X	X		X		X.	X
Barite	X	X	X	X	X			
Pyrite							X	X

of samples, abundances of some of the elements vary in a manner similar to their variation in roll-type deposits.

Vanadium and uranium

Figure 3 shows the maximum content of vanadium to be below the maximum uranium concentration. The concentration of vanadium is 15,000 ppm or 1.5 percent, whereas the maximum vanadium content of the roll-type deposits was found to be only about 1,500 ppm. If Harshman's concept of the migration or movement of elements in the formation of roll-type deposits can be extrapolated to tabular deposits such as the La Sal, the lower side of the ore layer with the high vanadium content would be the oxidized side of the "front," and the upper side of the uranium layer would be the reduced side.

Selenium

Like vanadium, selenium reaches its maximum concentration below the uranium layer (fig. 7). The maximum selenium concentration is 1,840 ppm in the La Sal suite, but the maximum selenium content in the roll-type deposits is about 1,000 ppm (Harshman, 1974). If the analogy of the roll-type deposits is applied to this tabular deposit, the oxidized side is below the uranium layer. Unlike the toll-type deposits, however, the selenium content does not seem to be an order of magnitude greater in the altered side than in the unaltered side. This variation may be a result of the limited distance away from the ore that samples were available. In the La Sal suite the selenium correlates very well with the lead content, because the selenium is largely tied up in the lead selenide, clausthalite (table 3).

Molybdenum

Harshman (1974) showed that, in uranium roll-type deposits, the molybdenum content increases at some distance from the ore in the unaltered or reduced facies. In the La Sal suite, the molybdenum occurs in and above the uranium layer (fig. 8). This distribution, by analogy with the roll-type model, indicates that the zone above the ore is the
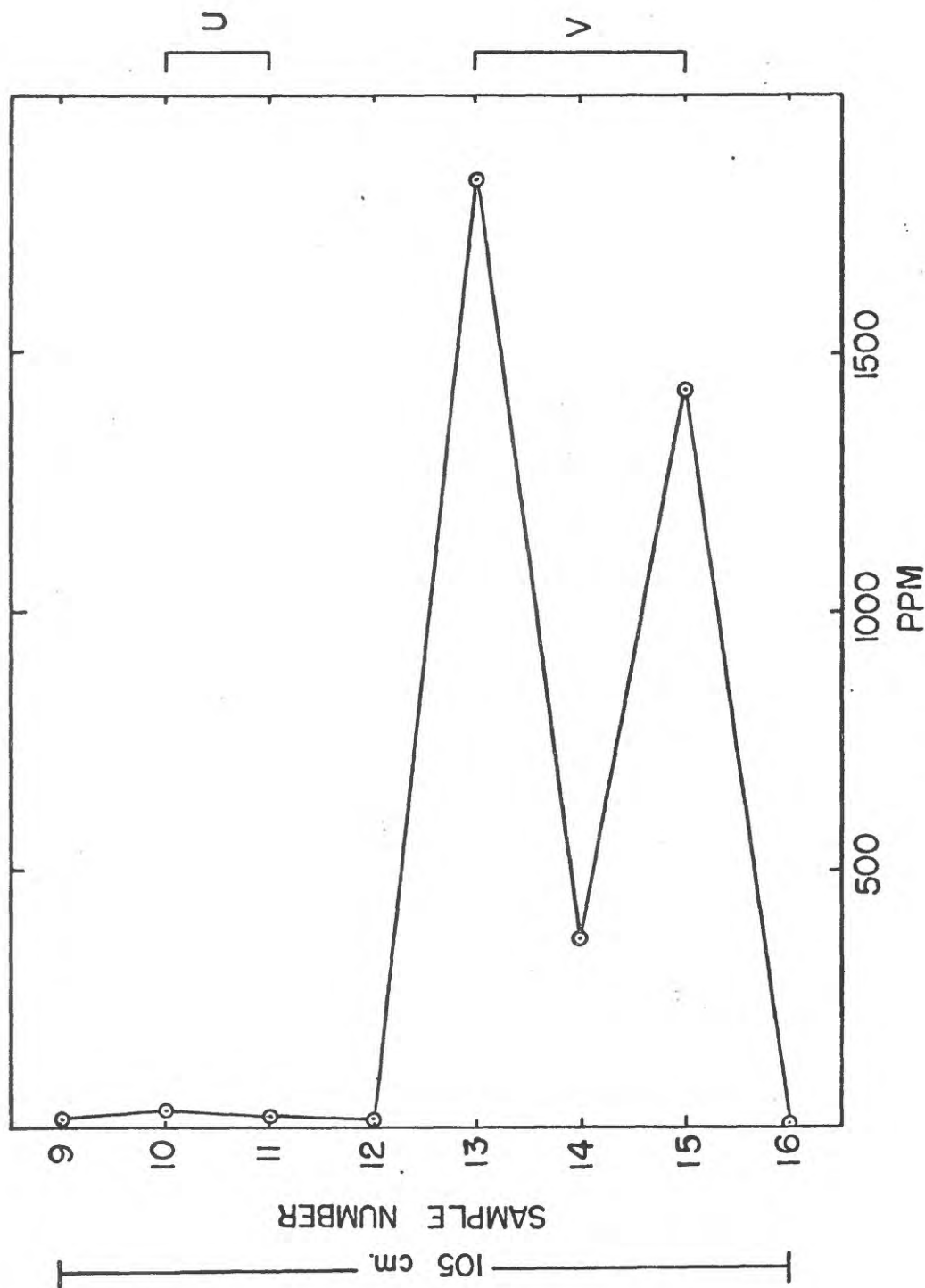
18

Figure 7.-- Selenium content of samples.

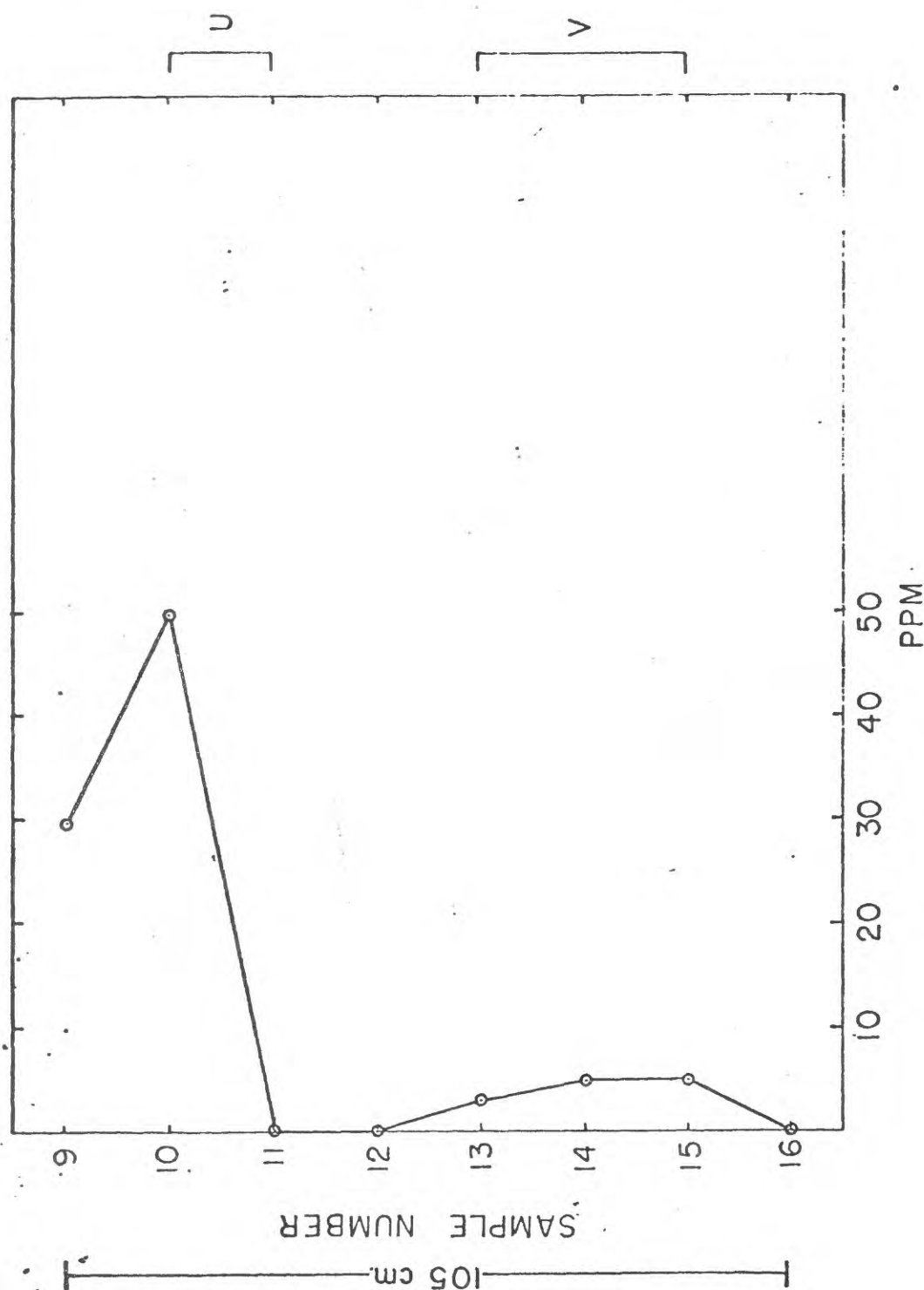Brackets refer to samples with maximum concentrations of uranium and vanadium. Samples taken over 105 cm interval.

Figure 8.--Molybdenum content of samples.
Brackets refer to samples with maximum concentrations of uranium and vanadium. Samples taken over 105 cm. interval.

20

unaltered or reduced facies. The maximum molybdenum content in the
La Sal suite is 50 ppm, whereas Harshman found molybdenum concentrations
as great as 1,000 ppm; however, this may be attributed to the limited
sampling.

Pyrite

Harshman (1974) also showed that the ferrous iron as pyrite was
higher in the unaltered facies than in the altered facies. Figure 9
shows that the iron content in the La Sal suite is greater below the
ore, or in the altered facies. However, in the La Sal suite, a
late-stage diagenetic event (fig. 10) added iron and makes the iron
content undiagnostic. Pyrite of several generations is present in all
samples.

Carbon

The distribution of organic and mineral carbon (fig. 11) shows
that the carbonate carbon is significantly greater both above and
below the ore layer. Most of the mineral carbon occurs as calcite, and
the calcium varies almost directly with the mineral carbon; organic
carbon, on the other hand, increases from 0.2 percent above the ore
to 0.8 percent within the vanadium zone and decreases to 0.7 percent
below the ore zone.

Chromium

Chromium is low above the ore layer and strongly enriched below
(fig. 12). On the Colorado Plateau, chromium-rich zones are quite
common in ores of the Entrada and Navajo Formations, but are uncommon
in the Morrison Formation (H. C. Granger, oral commun., 1974). The
regular distribution of chromium in the Navajo sandstone ores was
discussed by Fischer (1960). Anomalous chromium has not been reported
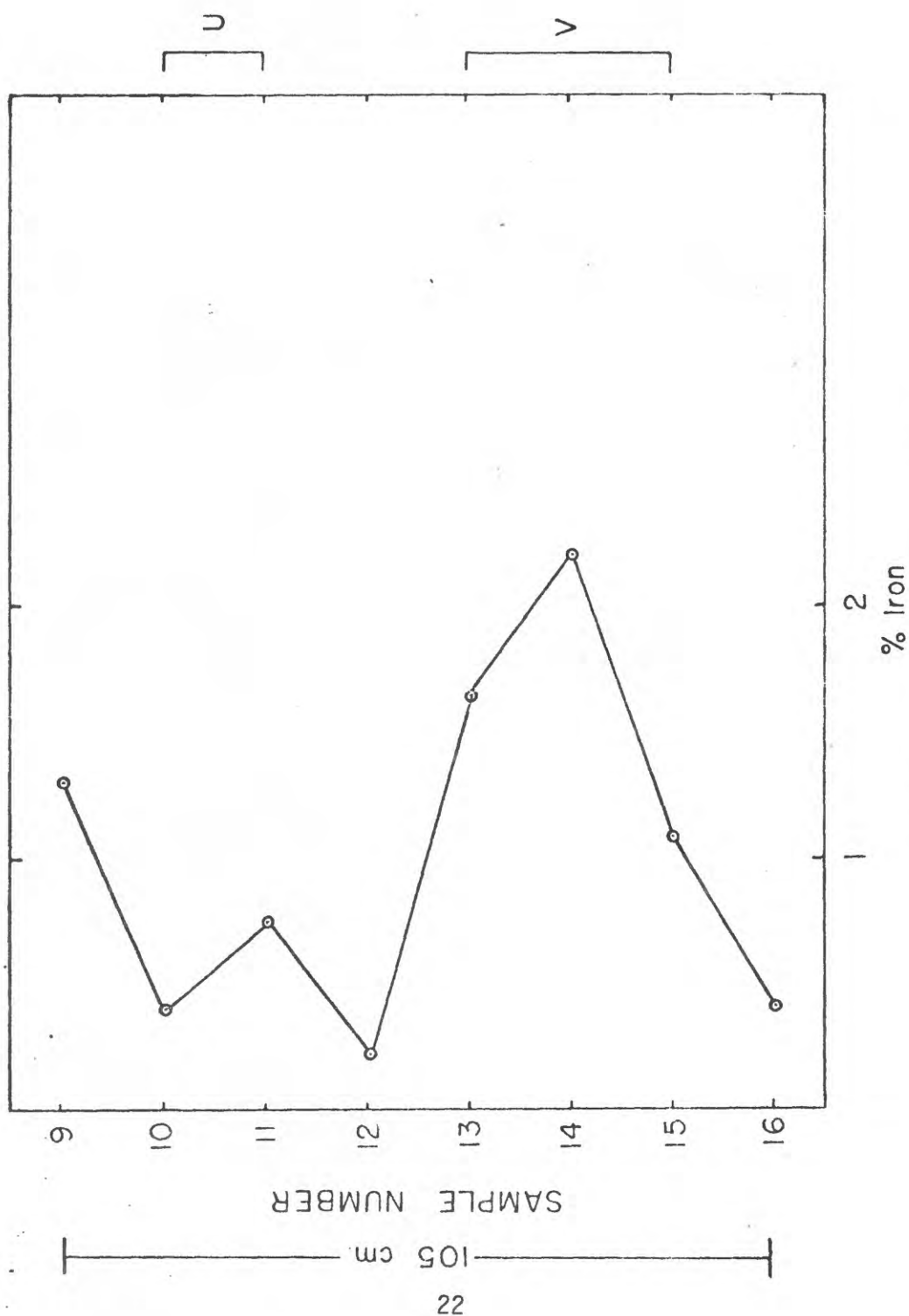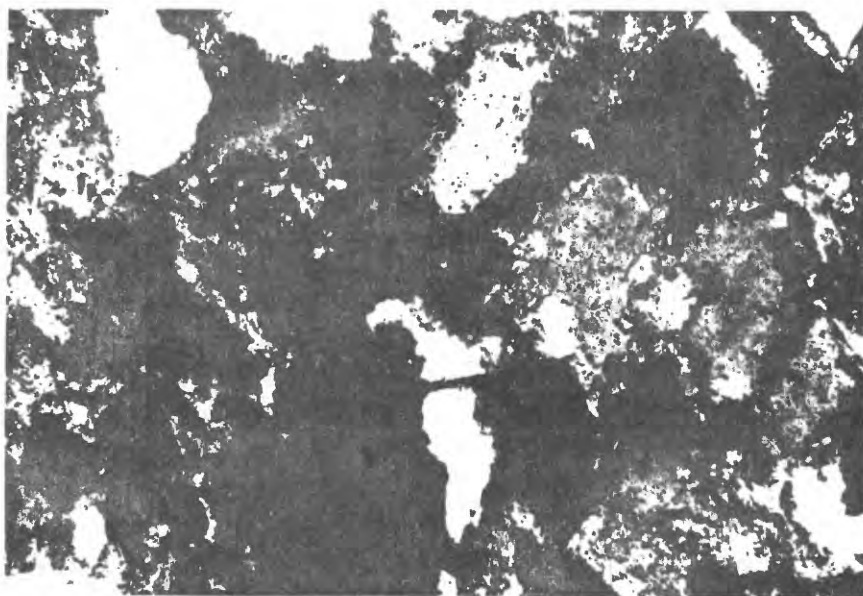in the roll-type deposits of Texas and Wyoming.

21

Figure 9.--Iron content of samples. Brackets refer to samples with maximum concentrations of uranium and vanadium. Samples taken over 105 cm interval.

Figure 10.--Late-stage pyrite formation. (Pyrite is
black mineral corroding quartz grain, 25X.)

Figure 11.--Carbon content of samples. Samples taken with maximum concentrations of uranium and vanadium. Samples taken over 105 cm interval.

Brackets refer to samples with maximum concentrations of uranium and vanadium. Samples taken over 105 cm interval.
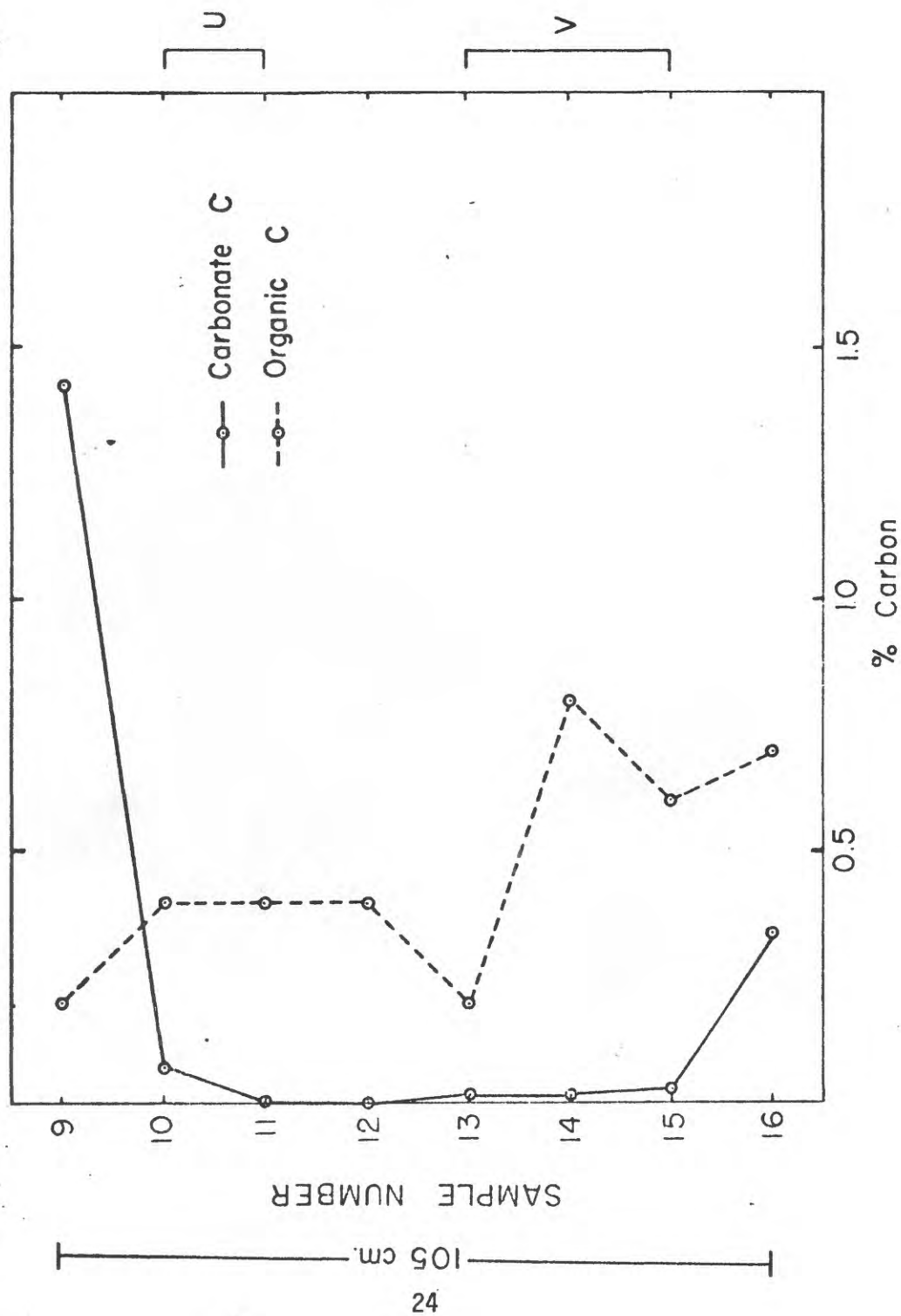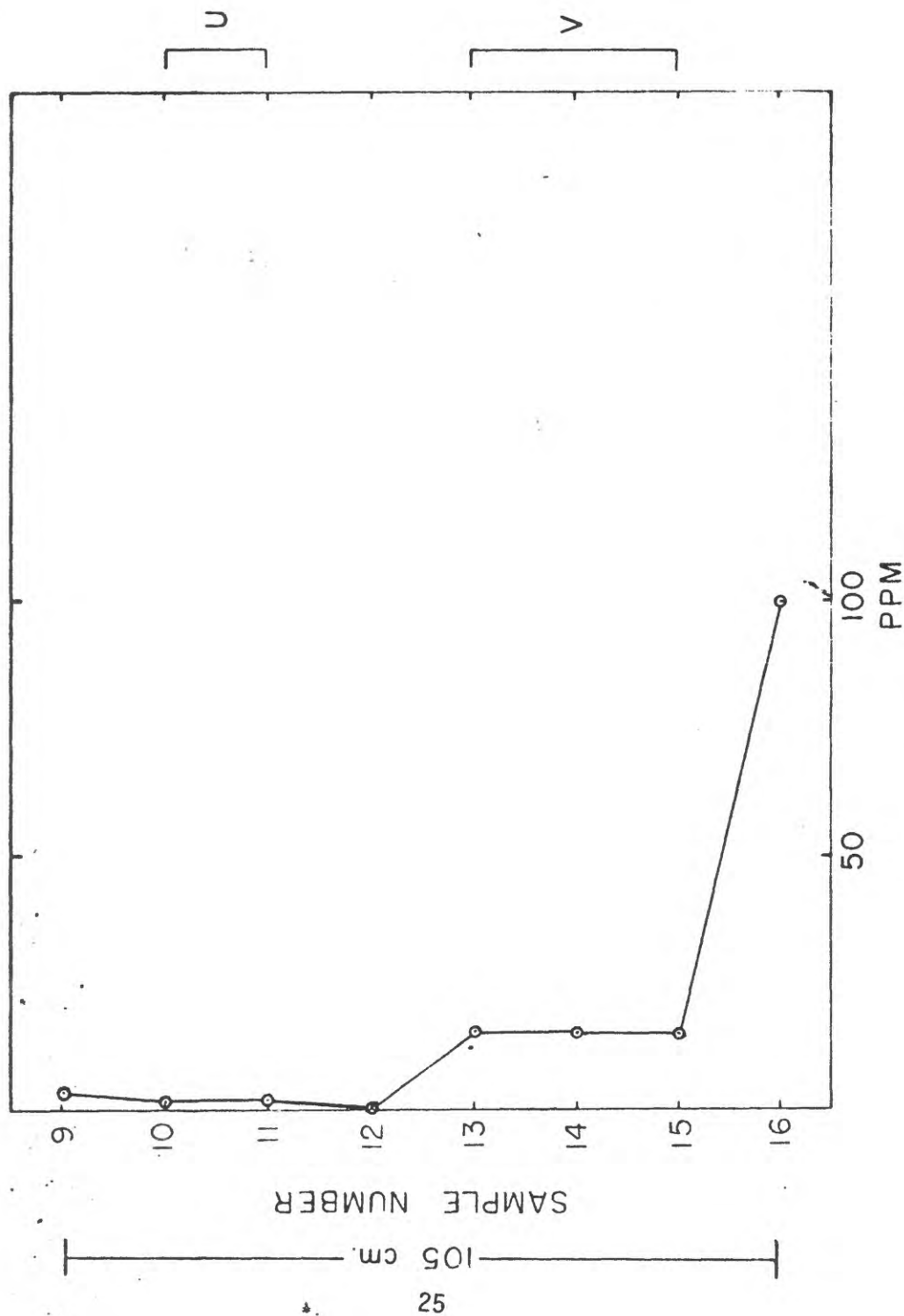
24

Figure 12.--Chromium content of samples.

Bracket refer to samples with maximum concentrations of uranium and vanadium. Samples taken over 105 cm interval.

25

Other elements

Barium and manganese are enriched in the upper part of the sample suite (fig. 13). Several other elements, including copper, cobalt, nickel, silver, titanium, boron, beryllium, yttrium, and scandium, are generally enriched in the vanadium-rich portion of the ore.

Lead concentration increases greatly in the vanadium-rich samples (fig. 14). This lead increase parallels the increase of selenium and is due to the presence of clausthalite ($PbSe_2$) in the vanadium zone.

Figure 13a.--Barium content of samples, uranium and vanadium. Samples taken over 105 cm interval.

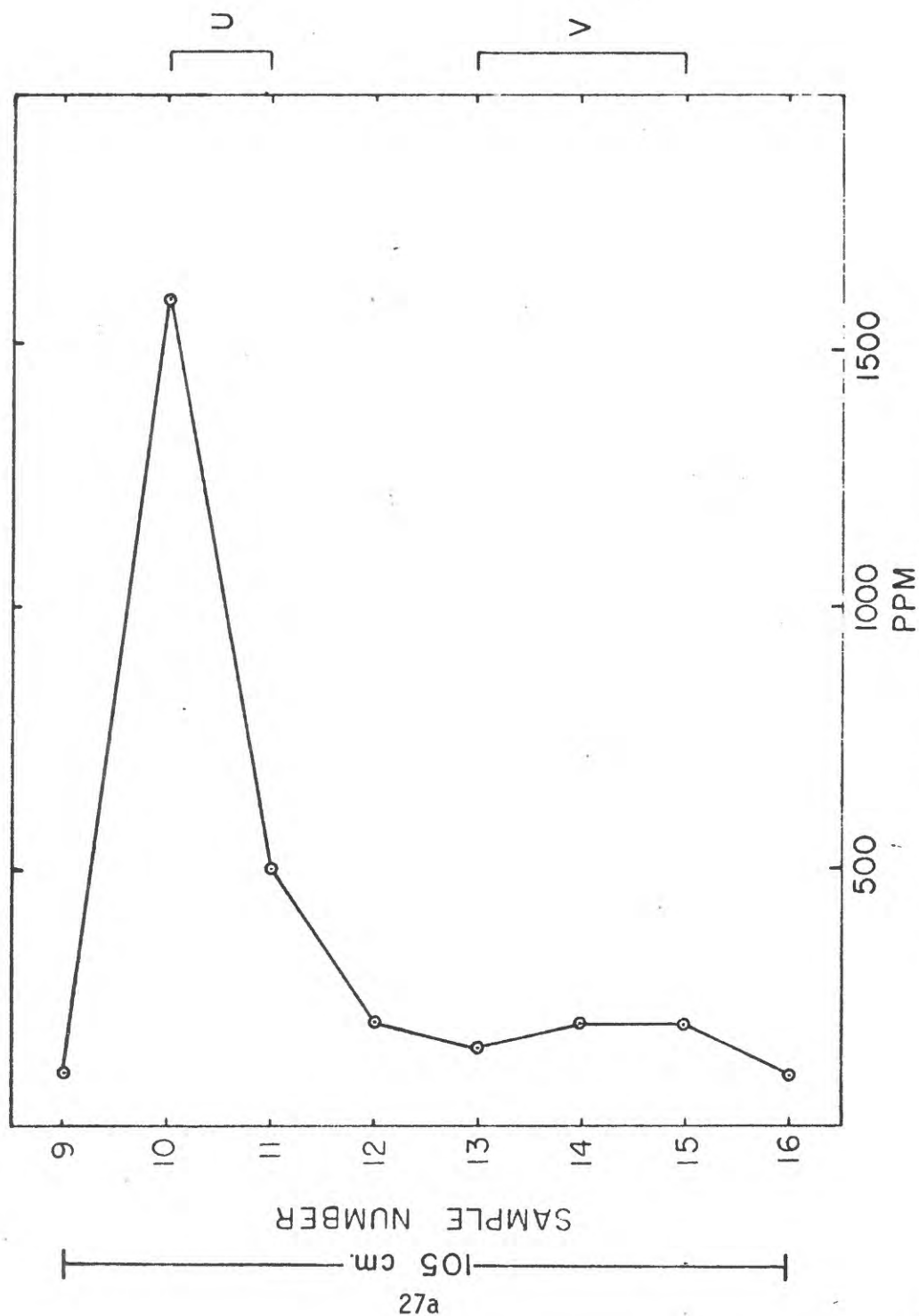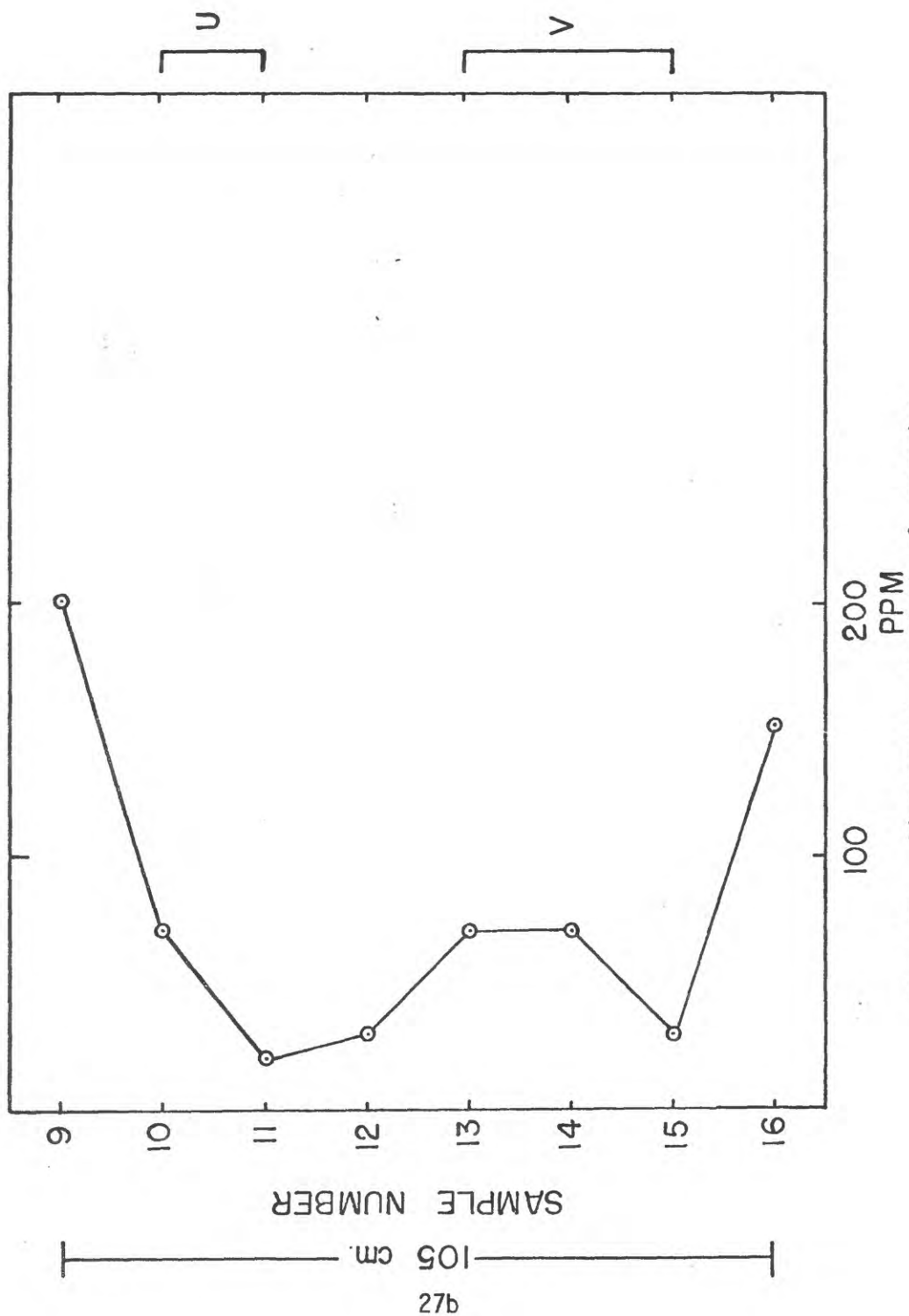Brackets refer to samples with maximum concentrations of uranium and vanadium.

27a

Figure 13b.-- Manganese content of samples.
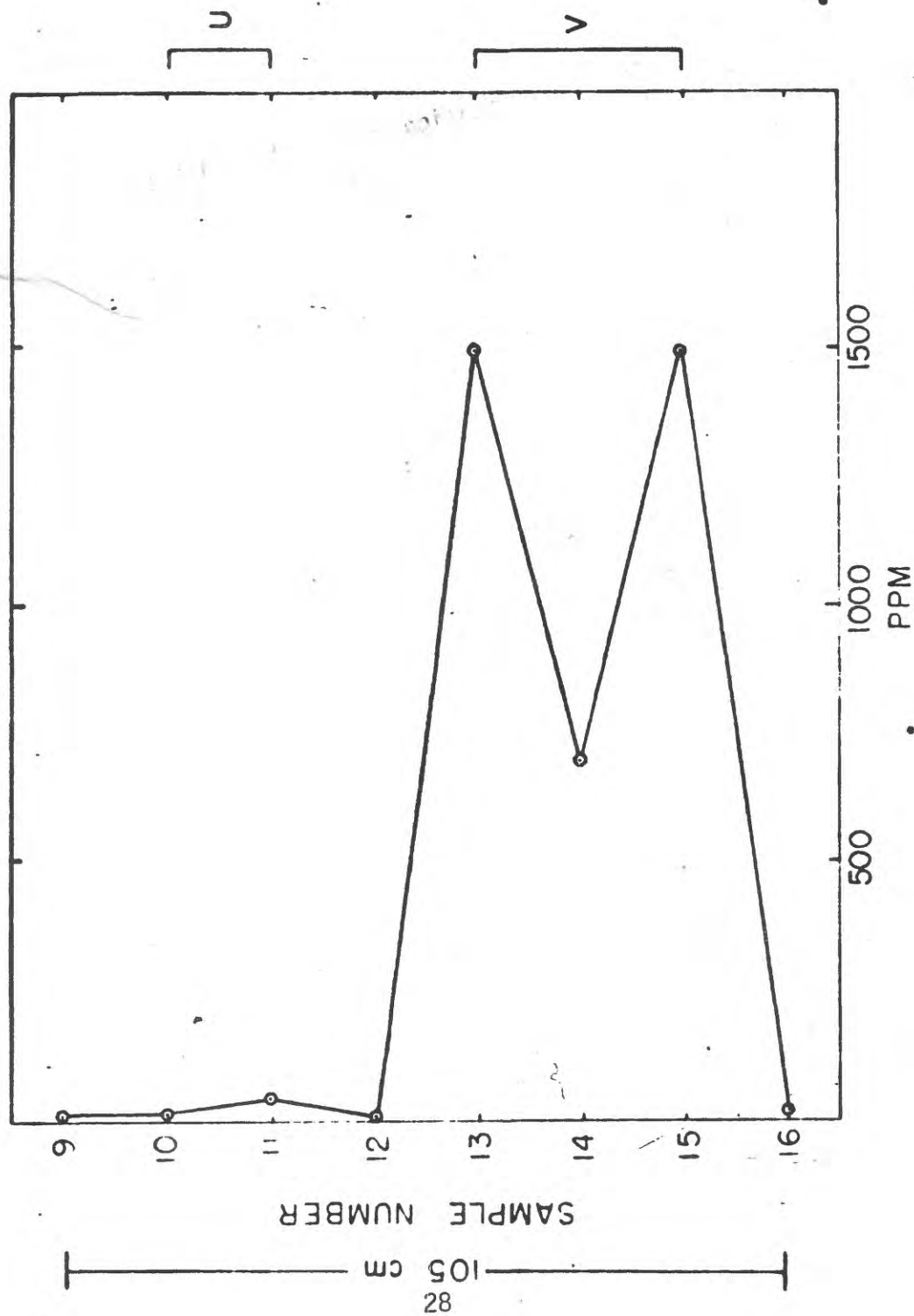Brackets refer to samples with maximum concentrations of uranium and vanadium. Samples taken over 105 cm interval.

27b

Figure 14.--Lead content of samples. Samples taken with maximum concentrations of uranium and vanadium. Samples taken over 105 cm interval.

Brackets refer to samples

28

SUMMARY OF RESULTS

1. Vanadium is concentrated in the dark-clay matrix, which constitutes visible ore. Uranium content is higher in the zone above the vanadium zone.

2. Calcium, carbonate carbon, and lead show greater than fifty-fold variations across the ore zone.

3. Copper and organic carbon show several-fold increase across the ore zone.

4. Elements that vary directly with vanadium content include magnesium, iron, selenium, zirconium, strontium, titanium, lead, boron, yttrium, and scandium.

5. Molybdenum occurs in and above the tabular layer.

6. Selenium occurs below the uranium zone within the richest vanadium zone.

7. Carbonate carbon is more abundant on both sides of the ore layer and depleted within it.

8. Iron is enriched in the vanadium zone.

9. Chromium is depleted from above the ore and strongly enriched below.

10. Barium and manganese are most abundant in the upper part of the zone.

11. The diagenetic sequence, as determined from thin sections, is as follows: (1) formation of secondary quartz overgrowths as cement; (2) the infilling and lining of remaining pores by amber quartz; (3) the formation of the dark-colored vanadium-rich clay matrix, which has replaced overgrowths as well as quartz grains. This event obscures all previous events in the richest vanadium ores; (4) introduction of calcite, replacing overgrowths and detrital grains and growing in amber material. This phase does not occur in the richest ore zones; (5) the infilling of pores with barite and the introduction of pyrite and marcasite.

12. The ore-forming processes produced the following textural and mineralogical changes in the sandstones: (1) marked increase in matrix content; (2) decrease in quartz overgrowths; (3) decrease in detrital grains, especially quartz, but also various rock fragments; (4) decrease in carbonate content.

References cited

Cadigan, R. A., 1967, Petrology of the Morrison Formation in the
    Colorado Plateau region: U.S. Geol. Survey Prof. Paper 556, 113 p.

Carter, W. D., and Gualtieri, J. L., 1965, Geology and uranium-vanadium
    deposits of the La Sal Quadrangle, San Juan County, Utah, and
    Montrose County, Colorado: U.S. Geol. Survey Prof. Paper 508, 82 p.

Fischer, R. P., 1960, Vanadium-uranium deposits of the Rifle Creek area,
    Garfield County, Colorado: U.S. Geol. Survey Bull. 1101, 52 p.

Hafenfeld, S. R., and Brookins, D. G., 1975, Mineralogy of uranium
    deposits northeast of Laguna District, Sandoval County, New Mexico:
    Am. Assoc. Petroleum Geologist Bull., v. 59, no. 5, p. 910-911.

Harshman, E. N., 1974, Distribution of elements in some roll-type
    uranium deposits, in Formation of uranium ore deposits: Internat.
    Atomic Energy Agency, Vienna, Proc. p. 169-183.

Hausen, D. M., 1959, Some mineralogical, textural and paragenetic relations
    in Salt Wash ore deposits in the Uravan area, Colorado; in National
    Western Mining and Energy Conference: Colorado Mining Assoc., 9 p.

Shawe, D. R., 1956, Significance of roll-orebodies in genesis of
    uranium-vanadium deposits on the Colorado Plateau, in Page, L. R.,
    Stocking, H. G., and Smith, H. B., compilers: U.S. Geol. Survey
    Prof. Paper 300, p. 239-241.

_____1966, Zonal distribution of elements in some uranium-vanadium
    roll and tabular orebodies on the Colorado Plateau: U.S. Geol.
    Survey Prof. Paper 550-B, p. 169-175.

_____1968, Petrography of sedimentary rocks in the Slick Rock District,
    San Miguel and Dolores Counties, Colorado: U.S. Geol. Survey Prof.
    Paper 576-B, 34 p.